The Separation of Copper and Nickel from Ni-Cu Mixed Ore Simulated Leaching Solution Using Electrochemical Methods

Razika Djouani, Qian Xu, Qiushi Song, Ying Chen

OPEN ACCESS
Eurasian Journal of Analytical Chemistry
ISSN: 1306-3057
2017 12(7):1015-1044
DOI: 10.12973/ejac.2017.00229a

The Separation of Copper and Nickel from Ni-Cu Mixed Ore Simulated Leaching Solution Using Electrochemical Methods

Razika Djouani
School of Metallurgy, Northeastern University, Shenyang 110819, CHINA
Qian Xu
State Key Laboratory of Advanced Special Steel, Shanghai University, Shanghai 200072, CHINA
Qiushi Song
School of Metallurgy, Northeastern University, Shenyang 110819, CHINA
Ying Chen
School of Metallurgy, Northeastern University, Shenyang 110819, CHINA

Received 5 June 2017 ▪ Revised 7 August 2017 ▪ Accepted 17 September 2017

ABSTRACT
Leaching solution of Ni-Cu mixed ore was studied using electrochemical methods to separate the two ions. This was observed through investigating the electrochemical behavior of copper and nickel ions separately in acidic mediums of copper sulfate and nickel sulfate solutions. To selectively deposit copper from Ni-Cu leaching solution, potentiostatic deposition was applied and the current efficiency was studied. At a voltage of – 0.2v the initial concentration of 3.6 g/l Cu^{2+} gradually reduced to 0.28 g/l was has no significant change for Ni^{2+} concentration. The reduction process of Cu^{2+} and Ni^{2+} also produced intermediate products of nickel hydroxide which formed at the surface of the current efficiency, especially when the concentration of Cu^{2+} is low.

Keywords: Cu-Ni leaching solution, electrochemical separation, potentiostatic deposition, cyclic voltammetry

INTRODUCTION

Copper is the world's third most widely used metal (after iron and aluminum). Its advantageous chemical, mechanical, and physical properties make it valuable in electrical and telecommunications products, building construction, industrial machinery and equipment, transportation, and consumer products. Copper's strategic uses include ordnance, command-communication-control-intelligence (C3I) systems, and military transportation and advanced weaponry systems. [1]

In order to produce the metal copper, a series of steps are involved where the final step is copper etectrowinning where copper metal is derived from oxide ores which have been

Correspondence: Razika Djouani, *School of Metallurgy, Northeastern University, Shenyang 110819, China.*
rzk12345@163.com

treated by sulphuric acid leaching. Nickel is also produced in many countries and is fast becoming a major demand in the last decades due to its anticorrosion properties [2]

Many scientific publications have been devoted to the description of copper and nickel determination in aqueous solutions. For example; atomic adsorption spectroscopy [3], high-performance liquid chromatography [4], and capillary electrophoresis [5], while atomic adsorption method offers good analytical performance in terms of precision and accuracy, it is nevertheless expensive considering its reagent consumption and instrumentation capital cost, but with the progress in science and technology and the improvement of environmental requirements, a more efficient and environmentally friendly separation process of copper and nickel is still a subject worthy of study.

The aim of this work is devoted to the recovery of copper from an optimized nickel-copper mixed solution, an approach is proposed based on simulated leaching solution using electrochemical methods, to provide theoretical basis and technical reference for the separation of the two ions.

This study is also very useful in the development of new technologies for the preparation of green metallurgy and alloy, the research is divided into two stages:

The first stage: the electrochemical behavior of Cu^{2+} and Ni^{2+} was analyzed separately in aqueous solution and also combining those both in a mixed solution using CV and SWV methods, and the kinetic parameters of the reaction mechanism have been investigated.

The second stage: the electrochemical behavior of the system was analyzed using potentiostatic methods to separate Cu^{2+} and Ni^{2+} from the mixed solution, and the experimental parameters such as: the quantity of charge, current efficiency and the edge of yield were investigated.

EXPERIMENTAL

Apparatus and Procedure

Electrochemical measurements were carried out using CHI model 660E. Where the electrochemical workstation was connected to a personal computer for control and data storage. All electrochemical experiments were performed in a standard three-electrode cell. The graphite electrode was used as the working electrode, graphite plate as the counter electrode and saturated calomel electrode (SCE) as the reference electrode. All potentials reported were plotted against the SCE.

Solution and reagents

The following table lists the experimental reagents and materials:

Table 1. Reagents and materials

Product name	Purity	Origin
$CuSO_4$	AR (249.69)	Tianjin kermel chemical reagent Co.Ltd
$NiSO_4$	AR (262.85)	Tianjin kwangfu fine chemical research institute
KCl	AR	Tianjin kermel chemical reagent Co.Ltd
H_2SO_4 (98%)	AR	Beijing chemical plant
Precision PH test paper	0.5-5	Shanghai san'aisi reagent Co.Ltd
Epoxy		Shenyeng multi value electronic technology research institute
Polyamide resin		Shenyang multi value electronic technology research institute
Sand paper	#400, #1000, #2000	Huizhou city ruifeng abrasive material Co.Ltd
Graphite electrode		Sinosteel shanghai new graphite material Co.Ltd
Graphite plate		Shanghai carbon material factory

Laboratory equipment

The experimental equipment and instruments are shown in **Table 2**.

Table 2. Laboratory equipment

Equipment	Origin
CHI660E electrochemical machine	Shanghai chen hua instrument Co.Ltd
Electronic balance	Beijing Sartorius instrument system Co.Ltd
UNIPOL-830 grinding and polishing machine	Shenyang branch of crystal automation equipment Co. Ltd
Three electrode electrochemical cell	
232-Reference electrode	Suzhou zheng hao technology Co. Ltd

Experimental Work

The experiment process consisted of four parts: solutions preparation, electrode fabrication, electrochemical analysis, chemical analysis and electro deposition of Cu^{2+} ions.

Preparation of solutions

In order to avoid the influence of other factors, the study used a synthetic mixed solution of Cu^{2+} and Ni^{2+} where its concentration was close to a copper –nickel mixed ore leaching solution.

Preparation of the electrode

In this experiment, we used three electrodes: working electrode (WE), counter electrode (CE) and reference electrode (RE).

Working electrode and counter electrode were made from graphite connected with a copper wire (Ø= 2mm). In order to make an electrode with a good surface reproducibility its resistance must be between 0.3- 0.8Ω.

Working electrode:

1. Ø= 4 mm of graphite rod was placed into a plastic pipe where Ø= 15mm.
2. Then a curing agent (polyamide resin) from resin epoxy A and B with a mass ratio of 1:2 was also prepared.
3. The solution was then added to the graphite rod until complete solidification was achieved.
4. After that, the rod was cut into 2cm pieces and then using a polishing machine, the pieces were polished with a 400# sand paper.
5. Holes were punched into one side of the graphite electrode. Note that the diameter of the hole should be slightly smaller than the diameter of the copper wire.
6. Then copper wire was connected to the graphite rod and sealed with the epoxy resin which was used as the curing agent before (step 2).
7. After curing was the polishing process using 400#, 1000#, and 2000 # sand paper.
8. Finally, ethanol was used for ultrasonic cleaning for 5 min to remove the residue and other impurities.

After the working electrode was prepared the assembling of the electrochemical system was carried out as follows;

Assembly of the electrochemical system

To have a good working electrode, counter electrode and saturated calomel electrode (which is also the reference electrode), an electrochemical system was built.

In order to reduce the resistance of the solution, the position of the three electrodes in the electrochemical cell needed to be fixed. Also, a certain distance between the working electrode and the capillary tube of the reference electrode must be maintained.

When the potentiostatic measurement was carried out the working electrode was replaced by graphite plate electrode. **[6]**

Electrochemical, chemical analysis and potentiostatic

Electrochemical behavior of the two different systems copper and nickel was analyzed by electrochemical methods such as cyclic voltammetry and square wave voltammetry.

Based on the result of electrochemical analysis a constant deposition potential was applied on the electrode. After that 5ml of the solution was taken at each time and diluted to 100 ml for chemical composition analysis.

Basic Principles of the Experiment

Test of the electrochemical system

The primary concern for the relative location of the three electrodes in a cell was the minimization of the solution resistance. This was accomplished by keeping the tips of the three electrodes as close together as possible, not interfering with the current paths between one another. Close approach was especially critical for the reference and working electrodes. The solution resistance between these electrodes led to an iR drop that manifested itself as an error in the measured potential difference between them. In addition, the potentiostat is normally unable to electronically compensate for this resistance, as it can for the resistance between the reference electrode and the auxiliary electrode. A Luggin capillary arrangement is often employed, in which the RE is placed inside a tube drawn at the end to a fine capillary allowing very close positioning relative to the WE. In this experiment, the outer diameter of the capillary Luggin was pulled to 0.5 to 0.1 mm and the distance between the capillary tube and the WE was about 1 mm.

The second important concern involved the shape and size of the auxiliary electrode relative to the working electrode. The CE should be at least as large in area as the WE, and positioned symmetrically with respect to the WE so that the current density and potential experienced along its entire length was constant.

The experimental electrolytes were $CuSO_4$, $NiSO_4$ solutions which were mixed at different concentrations, and the electrochemical test was carried out using a CHI660I electrochemical potentiostat. All the potentials in this paper are referred to SCE.

RESULT AND DISCUSSION

Electrochemical Behaviors of Cu^{2+} and Ni^{2+} Ions

Electrochemical behavior of Cu^{2+} ions in acidic solution

The electrochemical behavior of Cu^{2+} in different concentrations was studied.

First, a series of different concentrations of $CuSO_4$ were prepared using $CuSO_4.5H_2O$, the concentrations used are shown in **Table 3**.

Table 3. Concentrations used in the experiment

Sample	1	2	3	4	5	6	7
$CuSO_4$[g/l]	9.588	6.392	5.114	3.196	1.918	0.639	0.320

In graph (A) the sweep starts at 0v then it goes towards the cathodic potential direction where the first reduction peak C_1 appeared which corresponded to the reduction of Cu^{2+} to Cu^{+} **[7-9]**

$$Cu^{2+} + e^{-} \longrightarrow Cu^{+} \quad (1.1)$$

When the potential reached -0.2~-0.3 v there was an obvious reduction peak C_2 due to the reduction of Cu^+:

$$Cu^+ + e^- \longrightarrow Cu \quad (1.2)$$

Concurrently Cu^{2+} ions have the ability to be reduced directly to Cu:

$$Cu^{2+} + 2e^- \longrightarrow Cu \quad (1.3)$$

H_2 started being released at -0.75v as indicated in the reaction below:

$$2H^+ + 2\,e^- \longrightarrow H_2 \quad (1.4)$$

When the scan reached -0.8v the process of the forward scan started: the peak a_1 appeared between 0.1~0.2v followed by the peak a_2 indicating copper oxidation.

Oxygen evolution reaction appeared at the position of the oxidation peak a_3:

$$O_2 + 4e^- + 4H^+ \longrightarrow 2H_2O \quad (1.5)$$

Graph (B) in other words illustrated the cyclic voltammetry of 6.396 g/l of $CuSO_4$ solution with PH=1 at scan rate of 100 mv/s. From this voltammogram, we can observe that in the negative scan process there was only one obvious reduction peak C_2` due to the reduction of Cu^{2+} to Cu, and the corresponding oxidation peak.

Comparing graph B with graph A it was obvious that the general shape of the voltammogram obtained was different and this could be due to:

- The reduction current peak was relatively small due to the presence of the intermediate substance Cu+ for a short time and with a small solubility.

Comparing graph B with graph A it was obvious that the general shape of the voltammogram obtained was different and this could be due to:

- Another reason may be due to the short range between the two reduction potential intervals:

$$Cu^{2+} + e^- \longrightarrow Cu^+ \quad (1.6)$$

$$Cu^+ + e^- \longrightarrow Cu \quad (1.7)$$

Furthermore, when the concentration of Cu^{2+} increased the two peaks unified to form one peak which was obvious in graph (B) that the half width of C_2`was larger than C_1 and C_2 in **Figure (A)**.

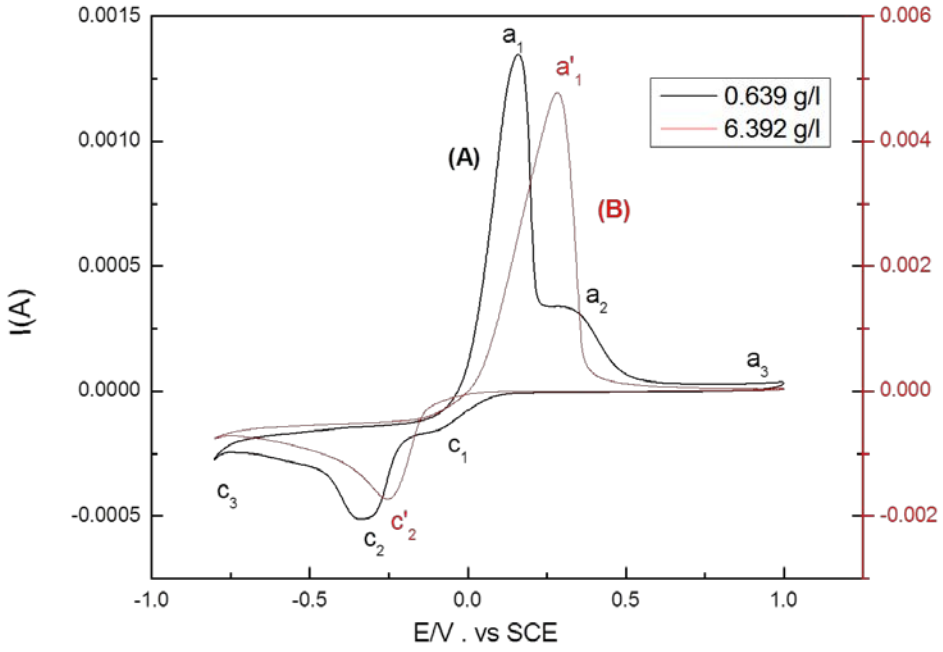

Figure 1. Cyclic voltammetry of (A) 0.639g/l of CuSO4 (B) 6.396g/l of CuSO4 at 100mv/s

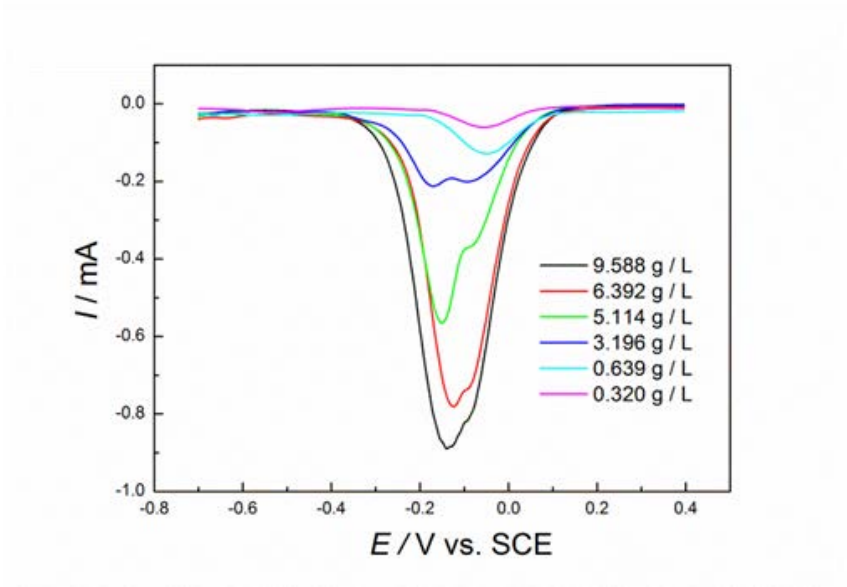

Figure 2. Square wave voltammetry curves of different concentrations of CuSO4 using graphite electrode at100 mv/s

Figure 2 illustrates the square wave voltammetry (SWV) curves of different concentrations of $CuSO_4$ solution on the graphite electrode.

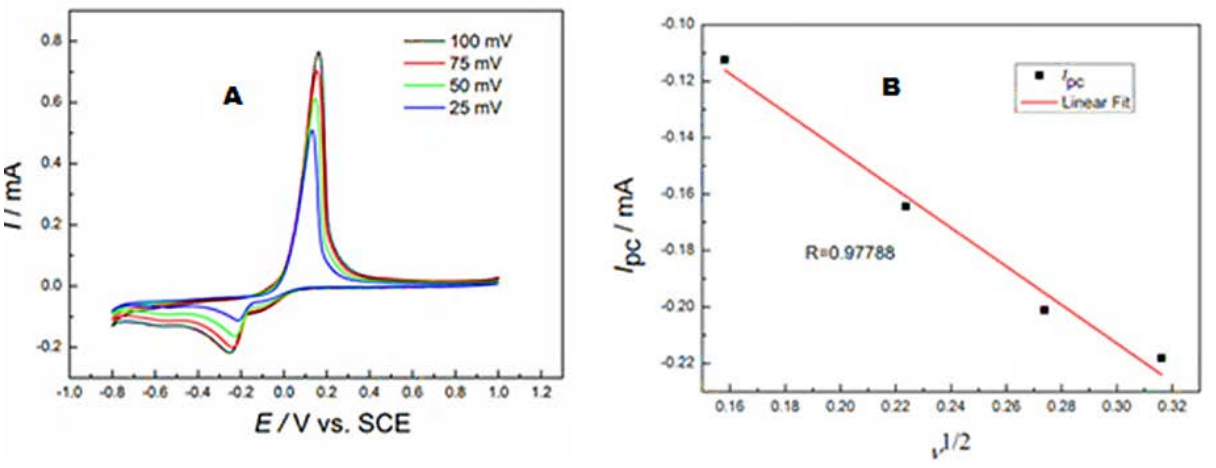

(A) (B)

Figure 3. (A) Cyclic voltammetry of0.639 g/l of CuSO4 at the graphite electrode using different scan rates. (B) Graph of cathodic peak vs the square root of the scan rate

From the figure, it can be seen that the reduction peak of Cu^{2+} appeared around 0~ -0.2v.

Since the SWV can eliminate the influence of the capacitance signal on the system the test results are more accurate and sensitive.

Compared to the cyclic voltammetry test results, the current intensity of the reduction peak measured by SWV was more obvious.

Two reduction peaks were found which proved that the reduction of Cu^{2+} reaction was a two-step process. In addition, the change of the electrode was observed after each scan as the color of the surface of the graphite electrode turned red from copper deposition.

Figure 3(A) and **4(A)** illustrates the cyclic voltammetry curves of 0.639g/l and6.392 g/l of $CuSO_4$ solution at different scan rates, it can be noticed that the peak current increased simultaneously with the increase of the scan rate.

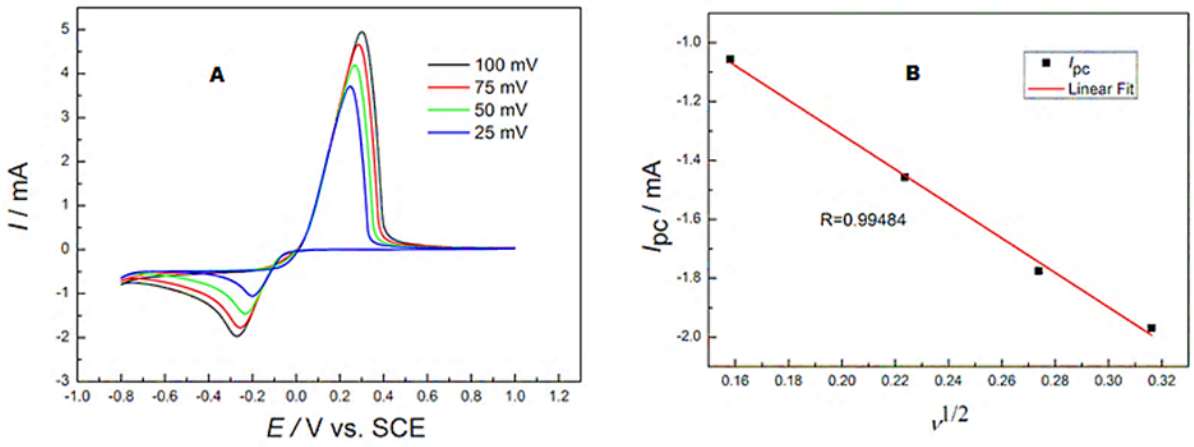

(A) (B)

Figure 4. (A) Cyclic voltammetry of6.392 g/l of CuSO4at the graphite electrode using different scan rates. (B) Graph of cathodic peak vs the square root of the scan rate

When the scan rate increased the reduction peak gradually shifted to the negative side and the oxidation peak shifted to the positive side.

On the other hand, **Figure 3(B)** and **4(B)** presented the linear fit of cathodic current peaks of low and high concentrations of $CuSO_4$ with the square root of the scan rate.

From the correlation degree of the curve it can be concluded that the linear relationship was very good, indicating that the process of Cu^{2+}/Cu electrode was mainly controlled by diffusion. It can be summarized that the Cu^{2+}/Cu process that occurred on the electrode surface in $CuSO_4$ solution was a quasi-reversible process controlled by diffusion.

From **Figure 5(A)** it can be seen that the current peak increased with the increase of the concentrations of Cu^{2+} ion in $CuSO_4$ solution, the reduction current peak appeared around -0.2~-0.3v and gradually shifted towards the negative side as the concentration increased.

In **Figure 5(B)** The graph of the current peak potential was plotted as a function of the concentration of $CuSO_4$, and the correlation degree R_1=0.99734, slope K_1=-0.294 was obtained. The graph played a very important guiding role in the electrochemical analysis of Cu^{2+} concentration at a certain concentration range.

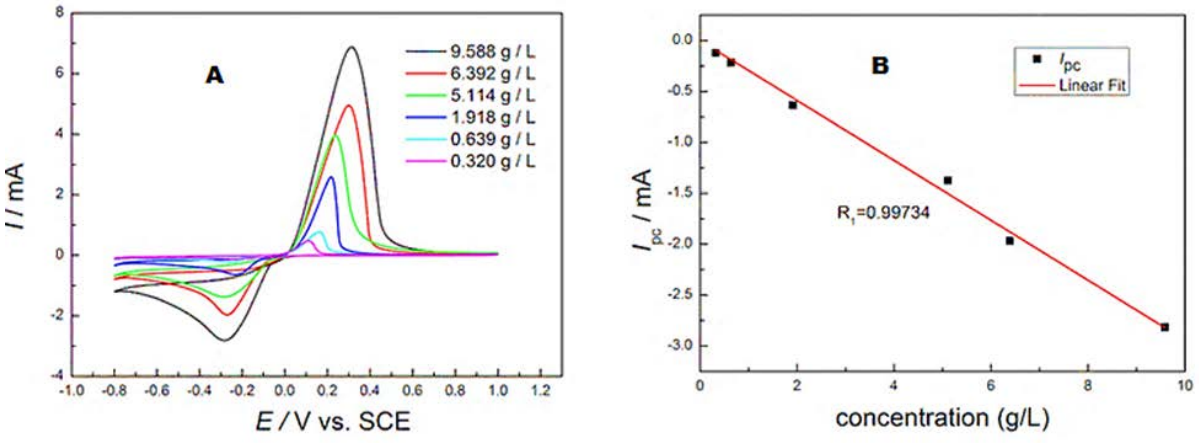

(A) (B)

Figure 5. (A) Cyclic voltammetry of different concentrations of CuSO4 at the graphite electrode at 100 mv/s (B) Graph of cathodic peak vs the concentration of CuSO4

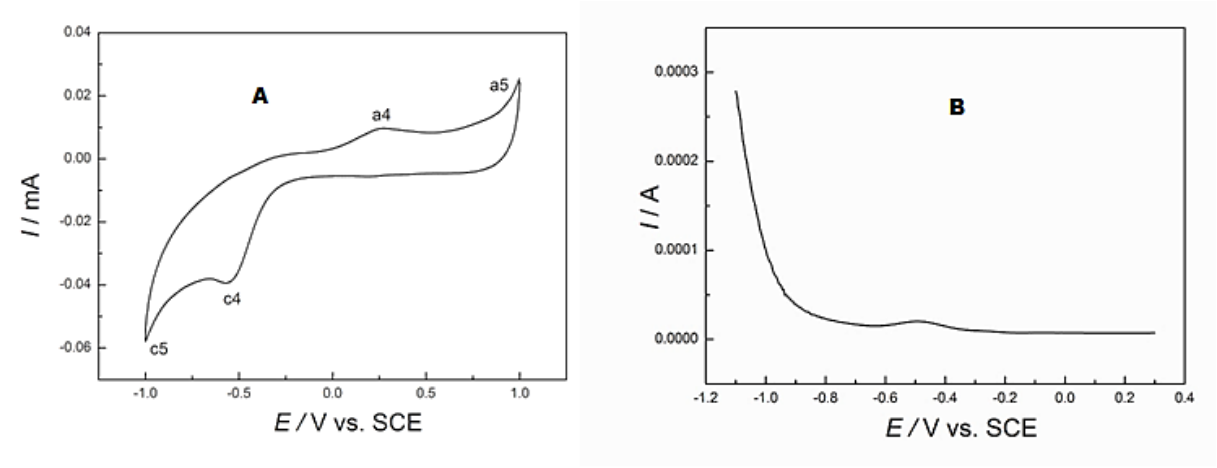

(A) (B)

Figure 6. (A) Cyclic voltammetry curve of 1.766 g/l ofNiSO4 solution at100mv/s. (B) linear sweep voltammetry of 1.766 g/l of NiSO4 solution at 100mv/s

Electrochemical behavior of nickel in acidic solution

Figure 6 shows the cyclic voltammetry curve of 1.766 g/l of$NiSO_4$ solution at 100mv/s.

From the graph, it can be seen that there are two reduction peaks, C_4 and C_5. The starting position of the current potential peak C_5 was –0.7v.

The possible reaction mechanism of nickel deposition as well as hydrogen discharge during nickel deposition can be suggested. The reaction pathway of Bockris et al. [10] was assumed to be most relevant for nickel deposition. In this mechanism all mentioned processes can be found.

This mechanism incorporates the nickel monohydroxide cation, $NiOH^+$, as an important species in the charge transfer. This monohydroxide was formed in the solution as a product of the first reaction step (1.8). In the next reaction step this species was adsorbed at the electrode (1.9), discharged (1.10) and the deposition of nickel at the electrode was the last reaction step (1.11). [11, 12]

$$\mathbf{Ni^{2+} + H_2O \leftrightarrow NiOH_{(aq)} + H^+} \quad (1.8)$$

$$\mathbf{NiOH_{(aq)} \leftrightarrow NiOH_{(ads)}} \quad (1.9)$$

$$\mathbf{NiOH_{(ads)} + e^- \rightarrow NiOH} \quad (1.10)$$

$$\mathbf{NiOH + H^+ + e^- \rightarrow Ni + H_2O} \quad (1.11)$$

Discharge of hydrogen also took place in several steps, **[13]** then two alternative mechanisms were possible. Hydronium cations (H_3O^+) were desolvated and partially discharged at the electrode surface (1. 11 a). In addition, their reaction with fresh nickel layer as catalysts were possible (1.11b).Next the hydrogen atoms combine in the adsorbed state to form adsorbed molecules (1.12 a, 1.12 b)

Then we have the desorption of adsorbed hydrogen molecules as bubbles as the last step in hydrogen discharge mechanism (1.13) as shown below;

$$\mathbf{H3O^+ + e^- \rightarrow H_{(ads)} + H_2O} \quad (1.11a)$$

or

$$\mathbf{Ni + 2H_3O^+ + 2e^- \rightarrow Ni\text{–}H_2 + 2H_2O} \quad (1.11b)$$

$$\mathbf{2H_{(ads)} \rightarrow H_{2(ads)}} \quad (1.12a)$$

or

$$\mathbf{2H_3O^+ + Ni\text{–}H2 + 2e^- \rightarrow Ni + 2H_{2(ads)} + 2H_2O} \quad (1.12b)$$

$$\mathbf{\mathit{n}H_2 \rightarrow (H_2)\mathit{n}} \quad (1.13)$$

Note that before, during and after each reaction in both mechanisms, the transportation of ions (Ni^{2+}, H_3O^+, $NiOH^+$, SO_4^{2-}, OH^-) from the bulk of solution to the diffusion layer or reversely can take place. In both processes, the nickel deposition and the hydrogen evolution occur simultaneously, and individual reaction steps can intersect [14].

The intermediate product may generate nickel metal Ni during further negative scan process.

It may also generate nickel ions Ni^{2+} which could be the reason of the low current efficiency during the process of potentiostatic measurement [15].

During the forward sweep of the potential two oxidation peaks appear:

The first peak A_4, corresponds to the oxidation of nickel metal Ni. The second one A_5, corresponds to the oxygen evolution reaction. (for more informations see appendix A)

Electrochemical behavior of Cu-Ni mixed solution

The electrochemical behaviors of Cu^{2+} and Ni^{2+} in aqueous solution were discussed. In this section the electrochemical behavior of Cu^{2+} and Ni^{2+} mixed solution in aqueous solution was studied, and the reduction and oxidation processes of the two ions were investigated.

The basic principle of the study was to maintain the same concentration of Ni^{2+} which was 2.944 g/l throughout the experiment while a series of different concentrations of $CuSO_4$ solution were prepared. The sulfuric acid was used to regulate the PH at 1.

The concentrations used in the experiment are presented in the following **Table 4**:

Table 4. Concentrations of solutions used during the experiment

Samples	**1**	**2**	**3**	**4**	**5**	**6**	**7**
$CuSO_4$/ g·L^{-1}	9.588	6.392	5.114	3.196	1.918	0.639	0.320
$NiSO_4$/ g·L^{-1}	2.944	2.944	2.944	2.944	2.944	2.944	2.944

The **Figure 7** represents the CV of the 8th sample before the deposition at 100v/s, the concentration of $CuSO_4$ and $NiSO_4$ was calculated according to the chemical analysis as follows: [$CuSO_4$]=1.356 g/l, [$NiSO_4$]= 2.832 g/l. Taking into account the large effect of hydrogen H_2 on the surface of the electrode, the scan range was adjusted to [0.8,-0.85v].

C_6 'corresponds to the Cu^{2+} reduction of Cu; C_7' corresponds to Ni^{2+} reduction, accompanied by hydrogen evolution (which is not obvious with this scan rate). Comparing **Figure 8** to **Figure 7**, it can be seen that when the Cu^{2+} concentration was low, two oxidation peaks a_8 and a_9 appeared, corresponding to the oxidation of nickel and copper peak respectively.

Figure 7 shows the cyclic voltammetry of 6.392 g/l of $CuSO_4$ and 2.944 g/l of $NiSO_4$ mixed solution at 100mv/s, the sweep scan range starts from 1v to -1 v. as it can be seen from the graph, the reduction peak C_6 appeared between -0.1 ~ -0.2v. by comparing the graph obtained with those obtained from the cyclic voltammetry curves of copper or nickel solution , it can be noticed that the magnitude of current potential peak of Ni^{2+} was twice as small as that of Cu^{2+}, therefore the C_6 position peak mainly corresponded to the process of reduction of Cu^{2+} to Cu metal.

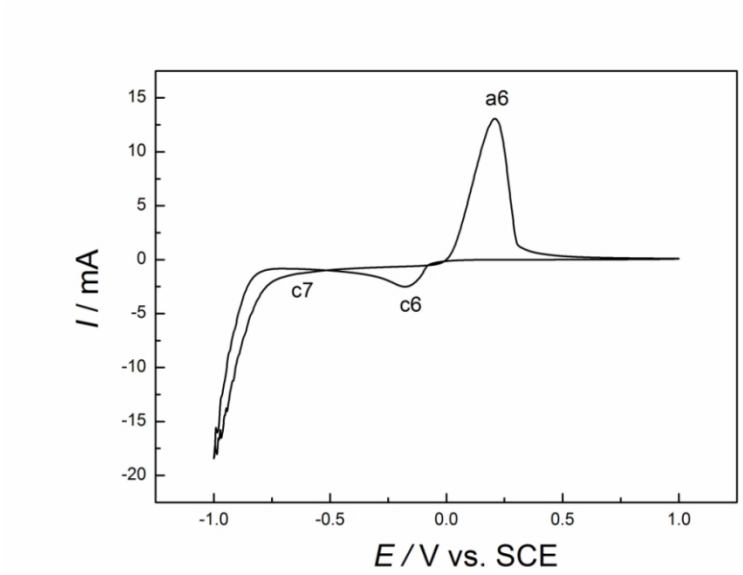

Figure 7. Cyclic voltammetry of 6.392 g/l of CuSO4 and 2.944 g/l of NiSO4 mixed solution at 100mv/s

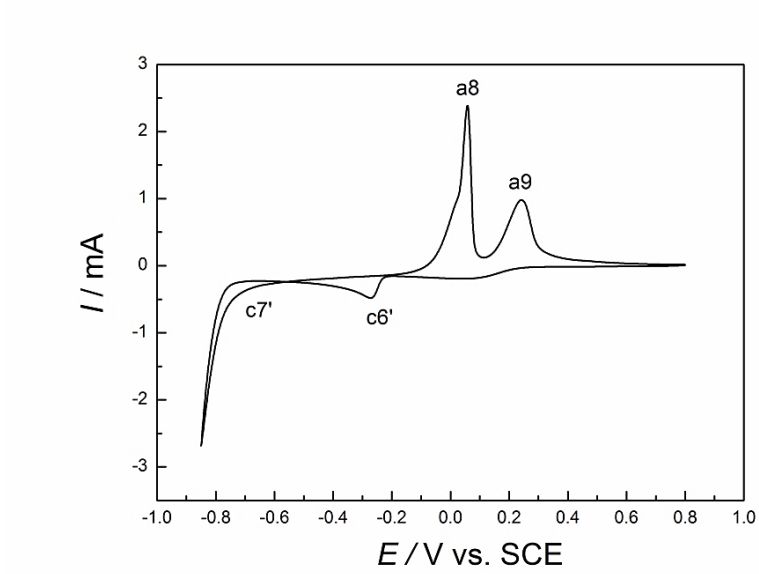

Figure 8. Cyclic voltammetry of the 8th sample before deposition at 100mv/s with a scan range [0.8, -0.85v]

If scan continued then the deposition of nickel would occur.

Under more negative potential the curve fluctuated that indicated the release of H_2.

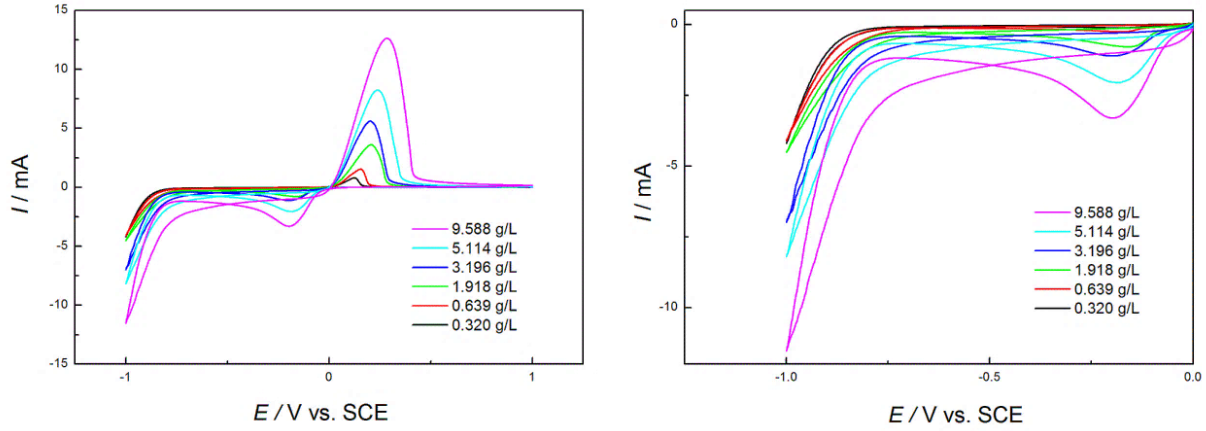

Figure 9. Cyclic voltammetry of different concentrations of CuSO4 and 2.944 g/l of NiSO4 in Cu-Ni mixed solution at 100mv/s

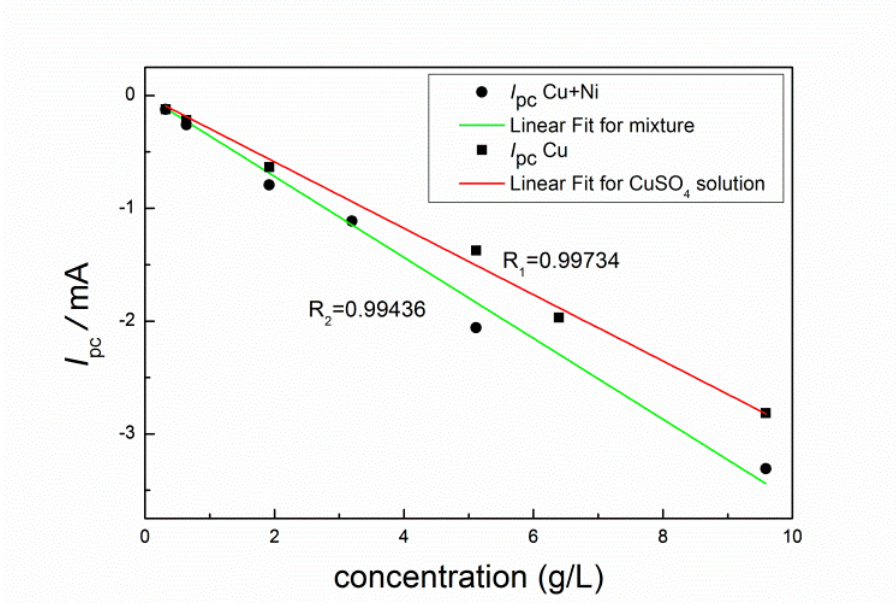

Figure 10. Comparison of linear fit of current cathodic potential peak in function of copper concentration in Cu-Ni mixed solution and copper solution

The **Figure 8** represents the CV of the 8th sample before the deposition at 100v/s, the concentration of $CuSO_4$ and $NiSO_4$ was calculated according to the chemical analysis as follows: [$CuSO_4$]=1.356 g/l, [$NiSO_4$]= 2.832 g/l. Taking into account the large effect of hydrogen H_2 on the surface of the electrode, the scan range was adjusted to [0.8,-0.85v].

C_6' corresponded to the Cu^{2+} reduction of Cu; **C_7'** corresponded to Ni^{2+} reduction, accompanied by hydrogen evolution (which was not obvious with this scan rate). Comparing **Figure 8** to **Figure 7**, it can be seen that when the Cu^{2+} concentration was low, two oxidation peaks **a_8** and **a_9** appeared, corresponding to the oxidation of nickel and copper peak respectively.

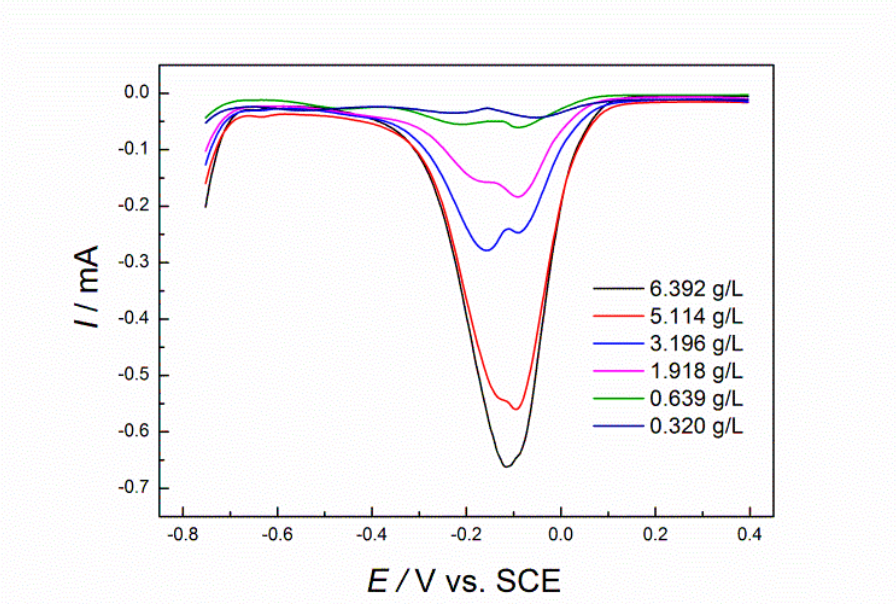

Figure 11. Square waves of different concentrations of CuSO4 and 2.944g/l of NiSO4 mixed solution

In **Figure 11** when the scan range was 0 to 0.5v it was seen that there was only one oxidation peak due to the low nickel reduction and oxidation current.

A significant difference between the two oxidation peaks of Cu^{2+} and Ni^{2+} could be made only in the presence of low concentration of Cu^{2+}; otherwise only one peak was formed.

Figure 9 represented the cyclic voltammetry of different concentrations of $CuSO_4$ and 2.944 g/l of $NiSO_4$ in mixed solution at 100mv/s. Around -0.1v a current peak appeare, it increased with the increase in Cu^{2+} concentration in the solution which proved that this peak had a relationship with the reduction of Cu^{2+}. According to the figure, it can also be seen that the deposition potential of Ni increased with the increase of Cu^{2+}, this was due to the prior deposition of Cu before Ni, in the reduction process of Ni^{2+}, and Cu^{2+} co-deposition and the reduction potential of Ni in Cu-Ni mixed solution was significantly higher and more positive than the reduction potential of Ni by itself.

This phenomenon was more obvious with the increase of Cu^{2+}concentration in the solution.

The correlation degree of the mixed solution is R_2=0.99436, and the slop is K_2=-0.359. Compared with the $CuSO_4$ solution alone, the absolute value of fitting curve slope in solution, which was under the same concentration had a greater current peak value. This was due to the existence of a certain amount of Ni^{2+} in the peak current caused by the reduction of intermediate products.

Potentiostatic Separation Study of Cu2+ and Ni2+

In order to ensure a big amount of deposition, we used 3cm * 4.5cm * 1cm graphite plate as a working electrode.

First, the chemical analysis of the initial deposition was set as a reference for the determination of copper and nickel concentration. After each deposition 5 ml was removed from the system and diluted 20 times for the chemical analysis of copper and nickel concentration.

Determination of the deposition potential

From the third measurement, it was known that the reduction of Cu^{2+} in the mixed solution of copper and nickel was about 0v, while nickel $Ni^{2+}$was deposited at about -0.7v.

Figure 11 shows the square wave voltammetry curve of different concentrations of $CuSO_4$ and 2.944g/l of $NiSO_4$ mixed solution. The potential reduction of Ni^{2+} and Cu^{2+} was obviously different. The separation of the two ions will be realized as long as the right electrode potential was applied, copper ions Cu^{2+} are reduced to Cu metal while Ni^{2+} ions still remained in the solution. The deposition of copper was studied by selecting a slightly negative constant potential -0.2V, -0.3 V.

Potentiostatic analysis process

Then we have the potentiostatic analysis process where 150ml of mixed solution that contains 9.588 g/l $CuSO_4$ and 2.944 g/l of $NiSO_4$ were prepared, where a constant potential of -0.2v,-0.3v (vs. SCE) was applied.

The series of potentiostatic analysis is presented respectively in **Table 5** below.

Table 5. Series of potentiostatic analysis

Samples	1	2	3	4	5	6	7	8	9	10
Deposition time /h	2	2	2	2	2	2	2	2	2	2

Figure 12 showed that the current was plotted as a function of time curved for the deposition process. As it can be seen from the figure the deposition current gradually decreased, and approached 0 with the increase in the deposition time. This must be due to the constant consummation of Cu^{2+} ions in the solution during the time which led to the decrease of the concentration.

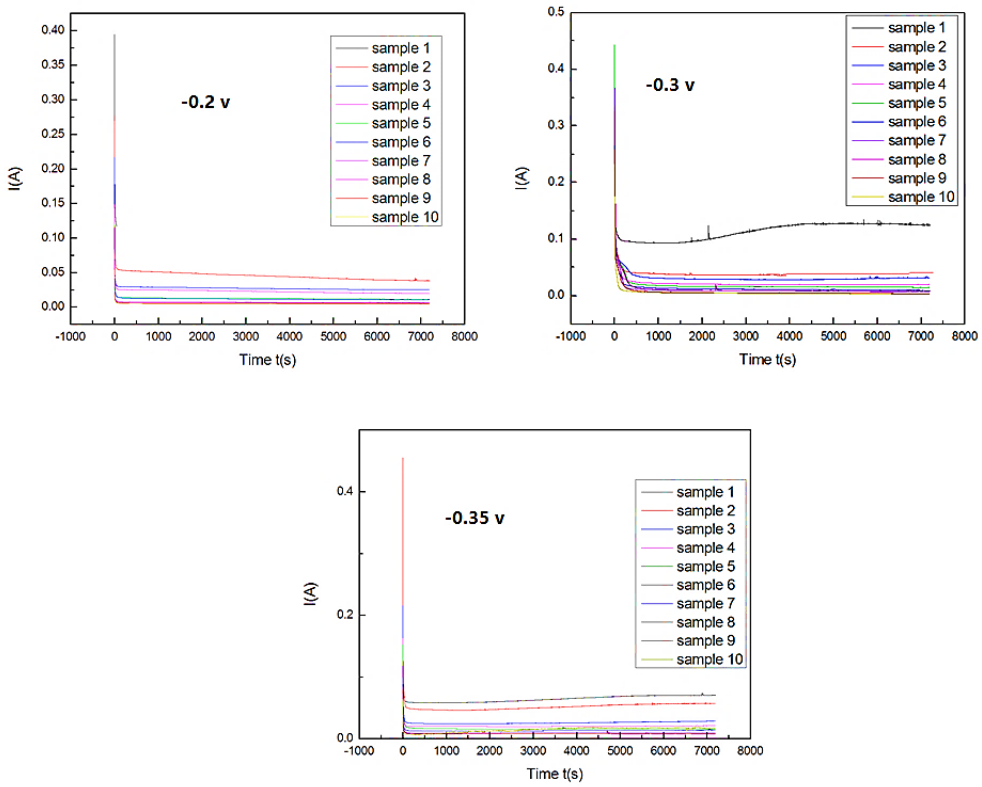

Figure 12. The Potentiostatic deposition *I-t*

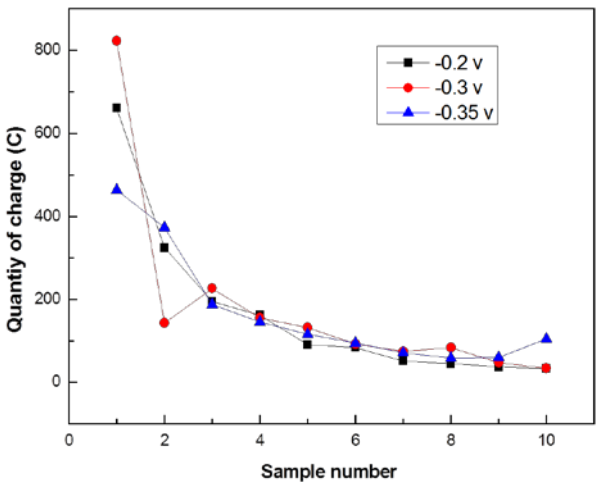

Figure 13. The electric charge consumed during the potentiostatic process at different voltages

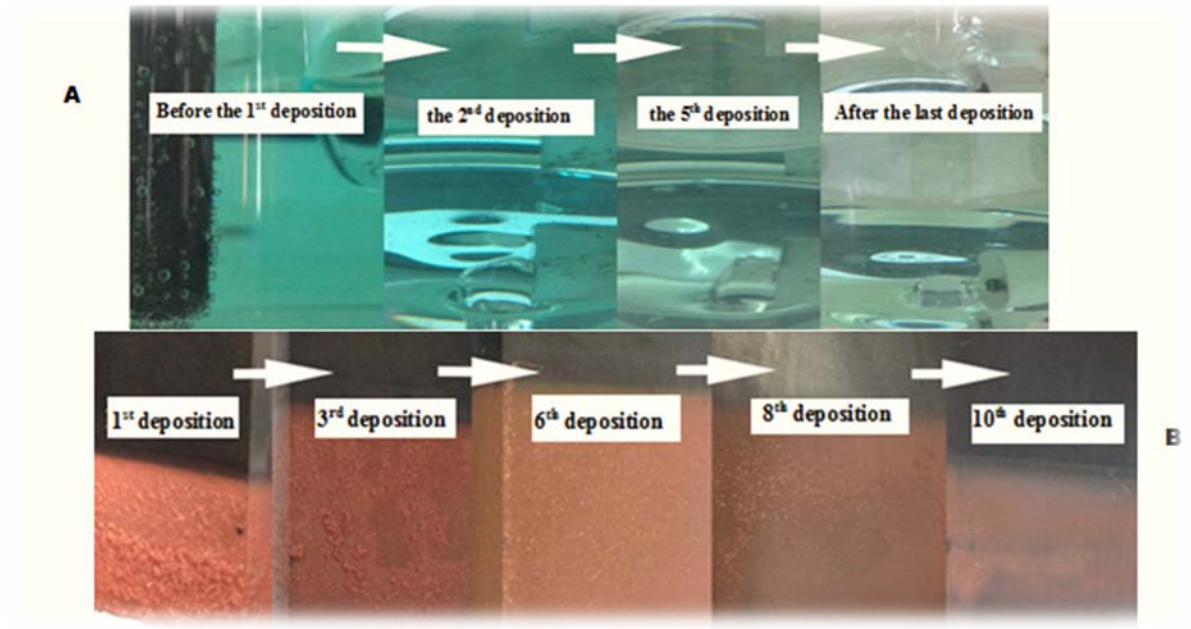

Figure 14. (A) The change in color of Cu-Ni mixed solution during the different stages of potentiostatic process analysis. **(B)** The deposition of copper metal during the different stages of potentiostatic process analysis.

Cu^{2+} ions were continuously reduced during the subsequent deposition Process.

Figure 14 (A) presents the change in color of Cu-Ni mixed solution during the different stages of potentiostatic process analysis.

As seen from the figure the color of the solution turned lighter as the deposition time increased, which indicates the gradual decrease of Cu^{2+} concentration.

At the same time, bubbles appeared on the surface of the electrode indicating the release of oxygen.

The change of the concentration of Cu^{2+} and Ni^{2+} in the mixed solution at different stages of deposition was found by chemical analysis methods. In the deposition process, the concentration of Cu^{2+} decreased gradually, after 20 hours of potentiostatic process, the concentration of the initial solution in the beginning was 3.60g/l, which finally decreased until it reached the lowest value 0. 284g/l when the potential was -0.2v. However, the concentration of Ni^{2+} did not change, which indicated that it was not reduced and almost all of it remained in the solution.

From the analysis above, it was shown that the potentiostatic method can effectively reduce the concentration of Cu^{2+} ion in Ni^{2+} and Cu^{2+} mixed solution, and the separation of the two ions is realized.

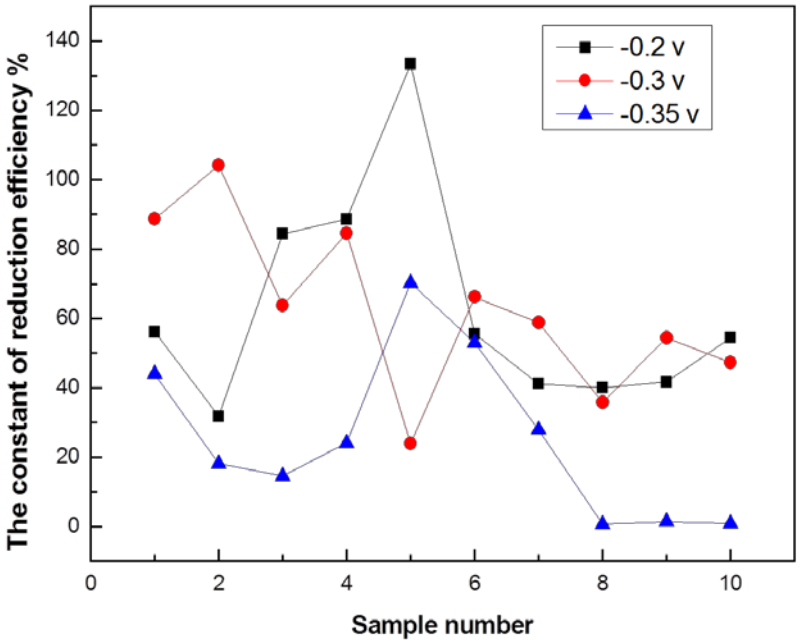

Figure 15. The reduction efficiency during the potentiostatic process at different voltages

The change in the concentration of the solution before and after the Deposition was calculated then compared with the amount of Cu^{2+} according to theory which (concentration) should be reduced. Finally, the reduction efficiency was obtained at different stages of the potentiostatic process, as it was shown in the **Figure 16** at the beginning of the deposition, the reduction efficiency was relatively high such as the first deposition efficiency was 88.66%. (See **Table 7**, **8**, **9**)

The concentration of Cu^{2+} decreased after each deposition while the deposition efficiency decreased gradually as well, where the lowest value reached was at 24%.

One of the possible reasons for this was that during the deposition process, not only the reduction process of Cu^{2+} to Cu occurred but also there was the formation of the intermediate products of copper and nickel.

As it is known, the intermediate products may reverse the reaction to regenerate Cu^{2+} and Ni^{2+}which would lead to the decrease of the current efficiency especially in low concentrations.

Table 7. Chemical analysis results at V= -0.2 v

Sample number	Volume (mL)	Deposition Time (h)	Quantity of charge (C)	Theoretical quantity of Cu deposited (mol)	Cu concentration ($g \cdot L^{-1}$)		Ni Concentration ($g \cdot L^{-1}$)		Experimental quantity of Cu deposited (mol)	Current efficiency (%)
					Before deposition	After deposition	Before deposition	After Deposition		
0	--	--	--	--	--	--	--	--	--	--
1	150	2	660.6	34.14×10^{-4}	3.6	2.38	1.1	1.07	19.19×10^{-4}	56.20
2	145	2	324.6	16.83×10^{-4}		2.04	1.07	1.09	5.35×10^{-4}	31.77
3	140	2	194.8	10.07×10^{-4}		1.504	1.09	1.09	8.49×10^{-4}	84.37
4	135	2	161.9	8.34×10^{-4}		1.504	1.09	1.09	7.39×10^{-4}	88.67
5	130	2	91.01	4.72×10^{-4}		1.032	1.1	1.1	5.66×10^{-4}	133.33
6	125	2	83.6	4.24×10^{-4}		0.518	1.1	1.1	2.36×10^{-4}	55.55
7	120	2	51.81	2.67×10^{-4}		0.456	1.1	1.1	1.10×10^{-4}	41.17
8	115	2	45.08	2.33×10^{-4}		0.39	1.1	1.1	0.94×10^{-4}	40
9	110	2	37.69	1.95×10^{-4}		0.34	1.1	1.1	0.78×10^{-4}	41.66
10	105	2	33.41	1.73×10^{-4}		0.284	1.1	1.1	0.94×10^{-4}	54.54

Table 8. Chemical analysis results V= -0.3 v

Sample number	Volume (mL)	Deposition Time (h)	Quantity of charge (C)	Theoretical quantity of Cu deposited (mol)	Cu concentration ($g \cdot L^{-1}$)		Ni Concentration ($g \cdot L^{-1}$)		Experimental quantity of Cu deposited (mol)	Current efficiency (%)
					Before deposition	After deposition	Before deposition	After Deposition		
0	--	--	--	--	--	--	--	--	--	--
1	150	2	822	42.60×10^{-4}	3.6	2	1.1	1.11	37.77×10^{-4}	88.66
2	145	1	143.7	7.45×10^{-4}	2	1.66	1.11	1.1	7.76×10^{-4}	104.18
3	140	2	226.7	11.75×10^{-4}	1.66	1.32	1.1	1.1	7.49×10^{-4}	63.76
4	135	2	155.1	8.04×10^{-4}	1.32	1	1.1	1.1	6.80×10^{-4}	84.58
5	130	2	131.5	6.81×10^{-4}	1	0.92	1.1	1.11	1.64×10^{-4}	24.02
6	125	2	91.8	4.76×10^{-4}	0.92	0.76	1.11	1.08	3.15×10^{-4}	66.17
7	120	2	74.3	3.85×10^{-4}	0.76	0.64	1.08	1.07	2.27×10^{-4}	58.85
8	115	2	83.9	4.35×10^{-4}	0.64	0.55	1.07	1.05	1.56×10^{-4}	35.88
9	110	2	47.7	2.47×10^{-4}	0.55	0.46	1.05	1.08	1.35×10^{-4}	54.5
10	105	2	34.6	1.79×10^{-4}	0.46	0.4	1.08	1.08	0.85×10^{-4}	47.34

Chemical analysis of the solution

Tables 7, **8** and **9** show the chemical analysis of the solution after each deposition.

After each deposition, the solution was analyzed using cyclic voltammetry method with a scan range [1,-1], as shown in **Figure 16**. From the graphs the reduction peak current of Cu^{2+} decreased with the decrease in the concentration.

When Cu^{2+} concentration was low, two oxidation peaks shifted towards the positive side, the oxidation peak appearing from 0.0 ~ 0.25 V corresponded to the oxidation of Ni and that appearing around 0.25~0.50 V corresponded to the oxidation of Cu.

Table 9. Chemical analysis results V= -0.35 v

* The concentrations in the tables are the results of chemical analysis

Sample number	Volume (mL)	Deposition Time (h)	Quantity of charge (C)	Theoretical quantity of Cu deposited (mol)	Cu concentration ($g \cdot L^{-1}$)		Ni Concentration ($g \cdot L^{-1}$)		Experimental quantity of Cu deposited (mol)	Current efficiency (%)
					Before deposition	After deposition	Before deposition	After Deposition		
0	--	--	--	--	--	--	--	--	--	--
1	150	2	463.3	33.33×10^{-4}	3.6	2.68	1.1	1.1	14.68×10^{-4}	44.04
2	145	2	373	26.83×10^{-4}	2.68	2.04	1.11	1.07	4.89×10^{-4}	18.22
3	140	2	187.1	13.45×10^{-4}	2.04	1.908	1.1	1.08	1.95×10^{-4}	14.49
4	135	2	145.2	10.43×10^{-4}	1.908	1.236	1.1	1.09	2.51×10^{-4}	24.06
5	130	2	115.2	8.28×10^{-4}	1.236	1.072	1.1	1.09	5.82×10^{-4}	70.28
6	125	2	94.83	6.81×10^{-4}	1.072	0.886	1.09	1.07	3.61×10^{-4}	53.01
7	120	2	71.65	5.51×10^{-4}	0.886	0.726	1.07	1.09	1.54×10^{-4}	27.94
8	115	2	58.81	4.22×10^{-4}	0.726	0.708	1.09	1.08	3.15×10^{-6}	0.74
9	110	2	60.33	4.33×10^{-4}	0.708	0.64	1.08	1.09	6.29×10^{-6}	1.45
10	105	2	104	7.47×10^{-4}	0.64	0.508	1.09	1.09	6.29×10^{-6}	0.84

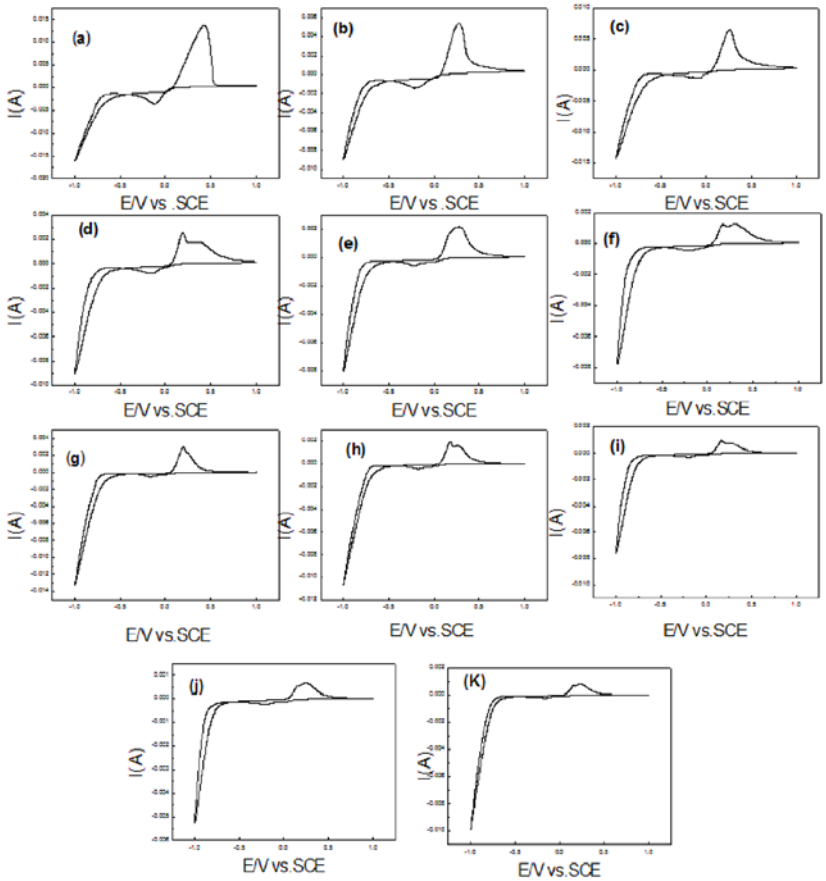

V=-0.2v

Figure 16. Cyclic voltammetry of Cu-Ni mixed solution after each deposition, from (a) to (k) respectively correspond to samples number used during the deposition process at scan rate 50mv/s

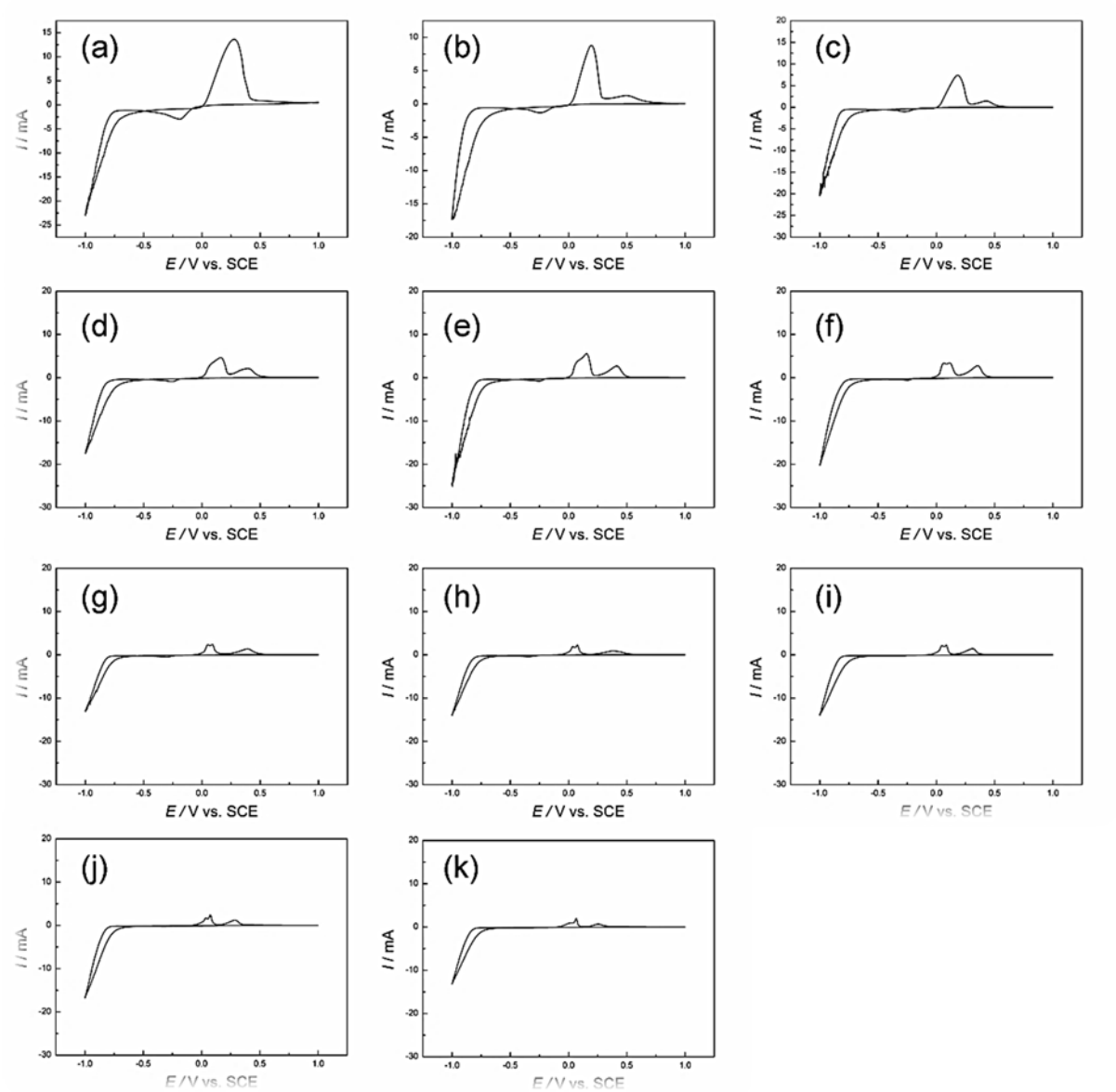

V=-0.3v

Figure 16 (continued). Cyclic voltammetry of Cu-Ni mixed solution after each deposition, from (a) to (k) respectively correspond to samples number used during the deposition process at scan rate 50mv/s

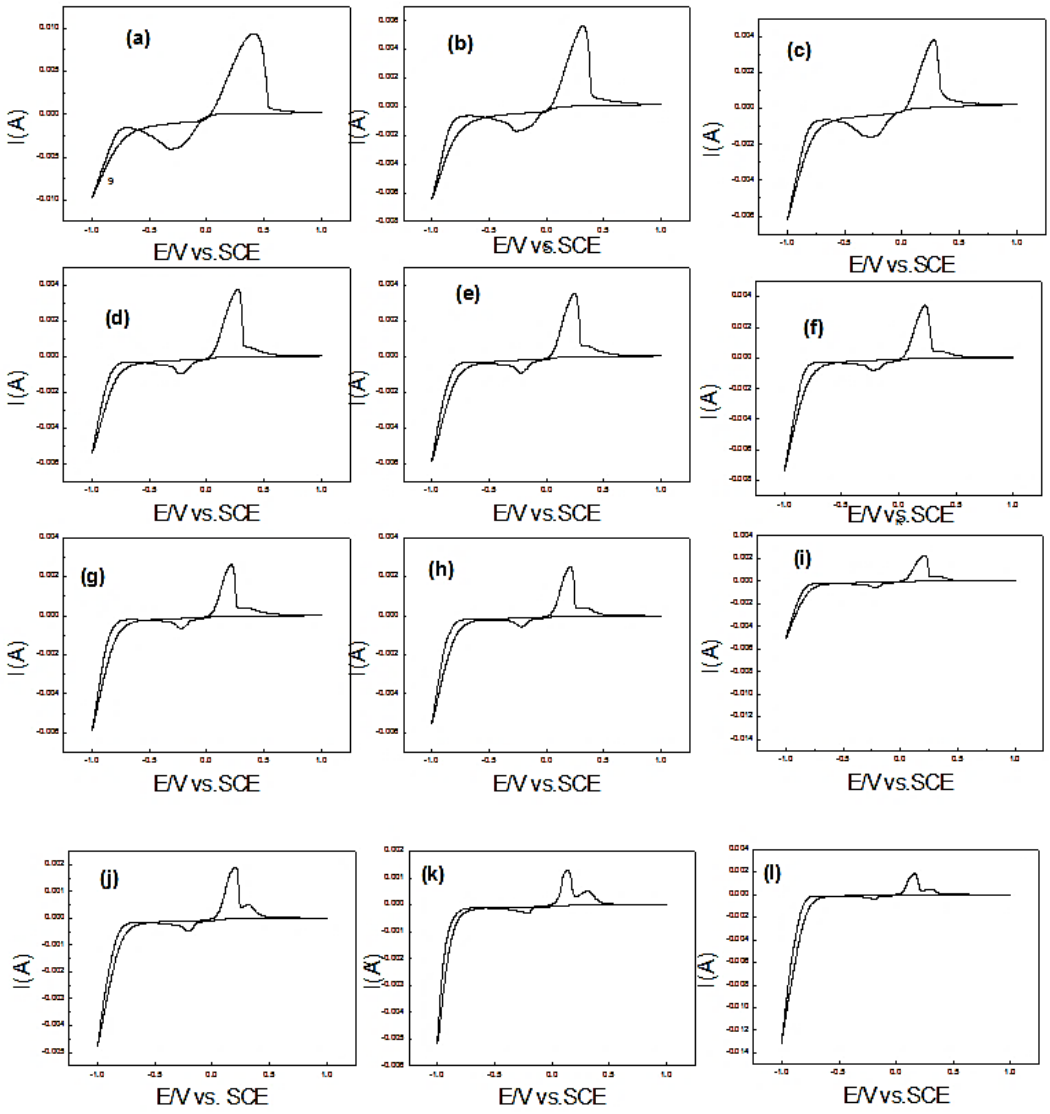

V=-0.35v

Figure 16 (continued). Cyclic voltammetry of Cu-Ni mixed solution after each deposition, from (a) to (k) respectively correspond to samples number used during the deposition process at scan rate 50mv/s

Using the same relationship between the concentration of the chemicals and the reduction peak current described in **Figure 3.9**, Cu^{2+} reduction peak current and the chemical analysis concentration of the deposition solution can also be analyzed.

XRD analysis of the electrode surface

The electrodes surface were characterized after the 1st and the 10th deposition respectively using XRD diffraction (see **Figure 17**).

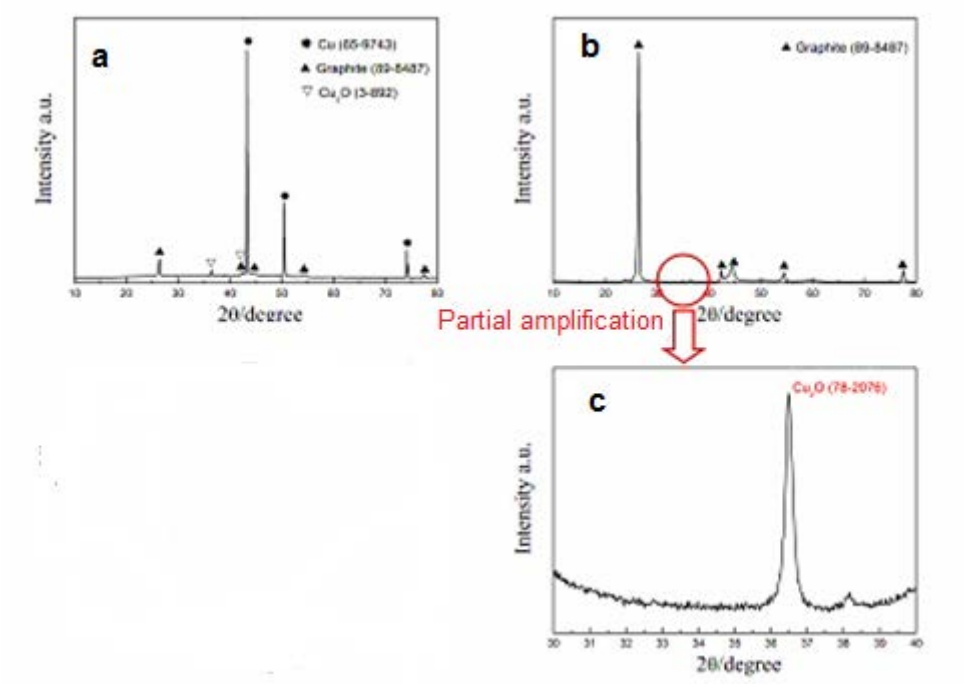

Figure 17. XRD diagrams of (a) 1th; (b) 10th deposition; (c) partial amplification of XRD diagrams of the 10th deposition

The surface of the electrodes consists of a large amount of red sediment of Cu, at the same time a certain amount of diffraction peak of Cu_2O can be detected.

The results above prove one more time (see the chemical analysis **Table 8**).

That only Cu and some of Cu_2O were deposited during the electrodeposition process while Ni^{2+} ions remained the same in the solution.

CONCLUSION

This study was the background of a new extraction technology of nickel ore.

Ni- Cu mixed leaching solution have been stimulated and studied using electrochemical methods: cyclic voltammetry (CV), square wave voltammetry (SWV) and potentiostatic analysis to study the electrochemical behavior of Cu^{2+} and Ni^{2+} ions.

Based on that, the potentiostatic method was used to separate the two ions electrochemically. The separation process and the current efficiency were studied, which provides the future research with theoretical and practical references for the separation of copper and nickel mixed ore leaching solution.

The main conclusions of the study are as follow:

1. In $CuSO_4$ solution, the reduction of Cu^{2+} simultaneously was a one-step reaction and step by step reaction. During the step by step reduction process, first Cu^{2+} was reduced to Cu^{+}, and then reduced to Cu, concurrently there are Cu^{2+} ions that were directly reduced to Cu.

Cu2+/Cu reaction was a quasi-reversible process controlled by diffusion.

The study of reduction current peak in function of Cu^{2+} ion concentration showed that the relationship between them was linear with a coefficient $\mathbf{K_1}$= -0.29427. In NiSO4 solution, the reduction potential of Ni^{2+} and H^{+} was very close. The Ni deposition is usually accompanied by the formation of the intermediate product such as **($NiOH^{+}$).**

2. The study of the electrochemical behavior of Cu^{2+} and Ni^{2+} mixed solution of a simulated leaching solution was done. Since there was a large difference of the deposition potential of the two ions, the separation between the two ions was easily achieved using potentiostatic method. Furthermore, the electrochemical peaks of the two ions were coupled together to form an envelope peak.

Cu^{2+} and Ni^{2+} would be co –deposited, which results in the deposition potential of Nickel to shift towards the positive potential direction. This phenomenon became more significant with the increase of Cu^{2+} concentration in the solution.

3. Cu^{2+} was deposited from the solution using potentiostatic method, while Ni^{2+} ion remained in the solution and the separation of the two ions was realized.

The initial concentration of Cu^{2+} in the solution was 3.60 g/l, and then gradually reduced to the lowest value 0. 284 g/l while the Ni^{2+} concentration remained the same in the solution.

During the reduction process of Cu^{2+} and Ni^{2+} the reduction and the decomposition of the intermediate products led to the decrease in the current efficiency, especially when the concentration of Cu^{2+} was low.

REFERENCES

1. U.S. Congress, Office of Technology Assessment. (1988). Copper: Technology and Competitiveness, (Washington, DC: U.S. Government Printing Office), OTA-E-367.
2. Coman, V., Robotin, B., & Ilea, P. (2013). Nickel recovery removal from industrial wastes: A review. Resources conservation and recycling, 73, 229-238.
3. Hwang, T. J., & Jiang, S. J. (1996), Determination of copper, cadmium and lead in biological samples by isotpe dilution inductively coupled plasma mass spectrometry after on line pretreatment by anodic stripping voltammetry, J. Anal. At. Spectrosc, 11, 353-357.
4. Das, R., Chakraborty, A. k., Cervera, M. L., & Delaguardia, M. (1996). Metal speciation in biological fluids: a review. Mikrochim, Acta, 122, 209.
5. Wen, J., & Cassidy, R. M. (1996). Anodic and cathodic pulse amperometric detection of metal ions separated by capillary electrophoresis. Anal. Chem., 68, 1047.

6. Liu, H.J., Xu, Q., Yan, C.W., Cao, Y.Z., & Qiao, Y.L. (2011). The effect of temperature on the electrochemical behavior of the V(IV)/ V(V) couple on the graphite electrode. International Journal of Electrochemical Science, 6, 3483.
7. Oliver-Tolentino, M. A., & Guzman-Vargas, A. (2013). Understanding electrochemical stability of Cu+ on zeolite modified electrode with Cu-ZSM5, Arce-Estrada, E. M. Journal of Electroanalytical Chemistry, 692, 31-39.
8. Nie, M., & Neodo, S. (2016). Electrochemical detection of cupric ions with boron – doped diamond electrode for marine corrosion monitoring, J.A. Wharton. Electrochimica Acta, 202, 345–356.
9. Reyna-González, J. M., Torriero, A. A. J., Siriwardana, A. I., Burgar, I. M., & Bond, A. M. (2010). Extraction of copper (II) ions from aqueous solutions with a methimazole- based ionic liquid. Anal. Chem, 82, 7691–7698.
10. Bockris, J. O. M., Drazic, D., & Despic, A. R. (1961). The electrode kinetics of the deposition and dissolution of iron. Electrochim. Acta, 4, 325.
11. Chassaing, E., Joussellin, M., & Wiart, R. J. (1983). The kinetics of nickel electrodeposition inhibition by adsorbed hydrogen and anions. J. Electroanal. Chem., 157, 75.
12. Wiart, R. (1990). Elementary steps of electrodepositon analysed by means of impedance spectroscopy. Electrochim. Acta, 35, 35.
13. Gabe, D. R. (1997). The role of hydrogen in electrodepositon processes. J. Appl. Electrochem. 27, 908.
14. Prasad, K. A., Giridhar, P., Ravindran, V., & Muralidharan, V. S. (2001). Zinc cobalt alloy: electrodeposition and characterization. J. Solid-state Electrochem. 6, 63.
15. Martínez, G. T., Zavala, G., & Videa, M. (2009). Electrodeposition of nickel particles and their characterization. J. Mex. Chem. Soc., 53(1), 7-11.

APPENDIX

Potentiostatic Analysis Process

In this part, we prepared 150 ml of mixed solution that contains 9.588 g/l

$CuSO_4$ and 2.944 g/l of $NiSO_4$, than a constant potential of -0.35v,-0.4v, -0.45 and -0.5 v (vs. SCE) were applied.

The change of the concentration of Cu^{2+} and Ni^{2+} in the mixed solution at different stages of deposition was found by chemical analysis methods.

During the deposition process, the concentration of Cu^{2+} decreased gradually, the solution turns gradually into black color.

If we take a look into the graphs we notice that there is no change in their shapes, which leads us to conclude that what have been deposited is Cu_2O

This part is an evidence that also the peak seen before (**Figure 6**) is not Ni deposition since Ni concentration did not change during the deposition process.

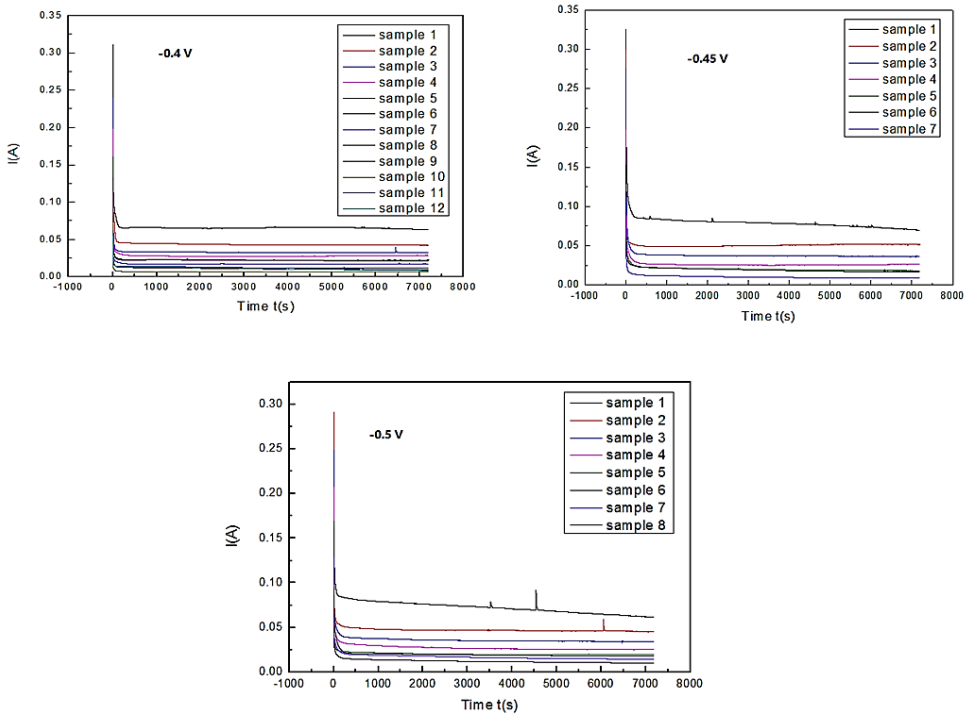

Figure 1. The Potentiostatic deposition *I-t*

Table 1. V= -0.4 V

Sample number	Volume (mL)	Deposition Time (h)	Quantity of charge (C)	Theoretical quantity of Cu deposited (mol)	Cu Concentration ($g \cdot L^{-1}$)		Ni Concentration ($g \cdot L^{-1}$)		Experimental quantity of Cu deposited (mol)	Current efficiency (%)
					Before deposition	After deposition	Before deposition	After Deposition		
0	--	--	--	--	--	--	--	--	--	--
1	150	2	473.3	24.51×10^{-4}	3.6	3.28	1.1	1.06	18.27×10^{-4}	74.54
2	145	2	312.8	16.19×10^{-4}		2.4	1.06	1.07	10.46×10^{-4}	64.60
3	140	2	243.9	12.59×10^{-4}		1.88	1.07	1.08	5.57×10^{-4}	44.24
4	135	2	200.6	10.39×10^{-4}		1.762	1.06	1.06	2.91×10^{-4}	28
5	130	2	162.8	8.43×10^{-4}		1.318	1.08	1.09	2.39×10^{-4}	28.35
6	125	2	85.48	4.42×10^{-4}		1.156	1.09	1.09	0.97×10^{-4}	21.94
7	120	2	124.5	6.44×10^{-4}		0.956	1.09	1.09	1.83×10^{-4}	28.41
8	115	2	157.4	8.15×10^{-4}		0.846	1.08	1.08	1.27×10^{-4}	15.58
9	110	2	74.46	3.85×10^{-4}		0.788	1.08	1.08	0.09×10^{-4}	2.33
10	105	2	46.97	2.42×10^{-4}		0.652	1.08	1.08	0.18×10^{-4}	7.43
11	100	2	84.12	4.34×10^{-4}		0.566	1.08	1.08	0.05×10^{-4}	1.15
12	95	2	76.34	3.95×10^{-4}		0.476	1.08	1.09	0.12×10^{-4}	3.03

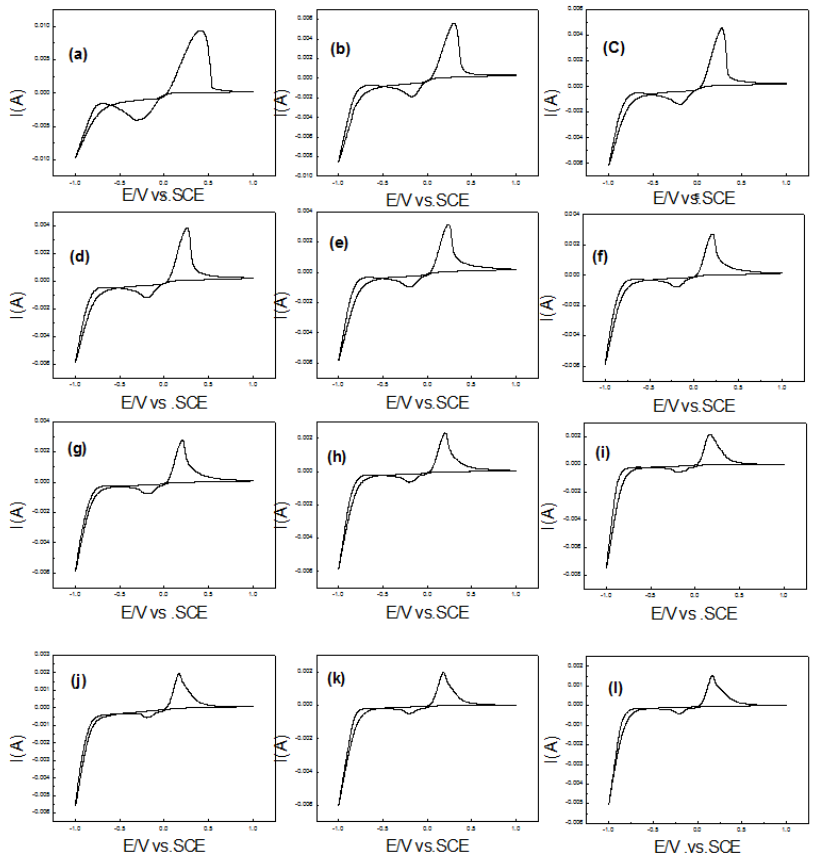

Figure 2. Cyclic voltammetry of Cu-Ni mixed solution after each deposition, from (a) to (l) respectively correspond to samples number used during the deposition process at scan rate 50mv/s

Table 2. V= -0.45 v

Sample number	Volume (mL)	Deposition Time (h)	Quantity of charge (C)	Theoretical quantity of Cu deposited (mol)	Cu concentration ($g \cdot L^{-1}$)		Ni Concentration ($g \cdot L^{-1}$)		Experimental quantity of Cu deposited (mol)	Current efficiency (%)
					Before deposition	After deposition	Before Deposition	After Deposition		
0	--	--	--	--	--	--	--	--	--	--
1	150	2	568.1	29.42×10^{-4}	3.6	3.06	1.1	1.07	30.37×10^{-4}	103.22
2	145	2	364.8	18.88×10^{-4}		2.46	1.07	1.05	23.85×10^{-4}	126.32
3	140	2	271.3	14.05×10^{-4}		1.688	1.05	1.06	9×10^{-4}	64.05
4	135	2	188.8	9.77×10^{-4}		1.314	1.06	1.07	8.35×10^{-4}	85.46
5	130	2	145.4	7.52×10^{-4}		0.932	1.07	1.09	4.57×10^{-4}	60.77
6	125	2	138.7	7.18×10^{-4}		0.822	1.09	1.07	3.41×10^{-4}	47.49
7	120	2	73.63	3.81×10^{-4}		0.648	1.07	1.09	2.36×10^{-4}	61.94

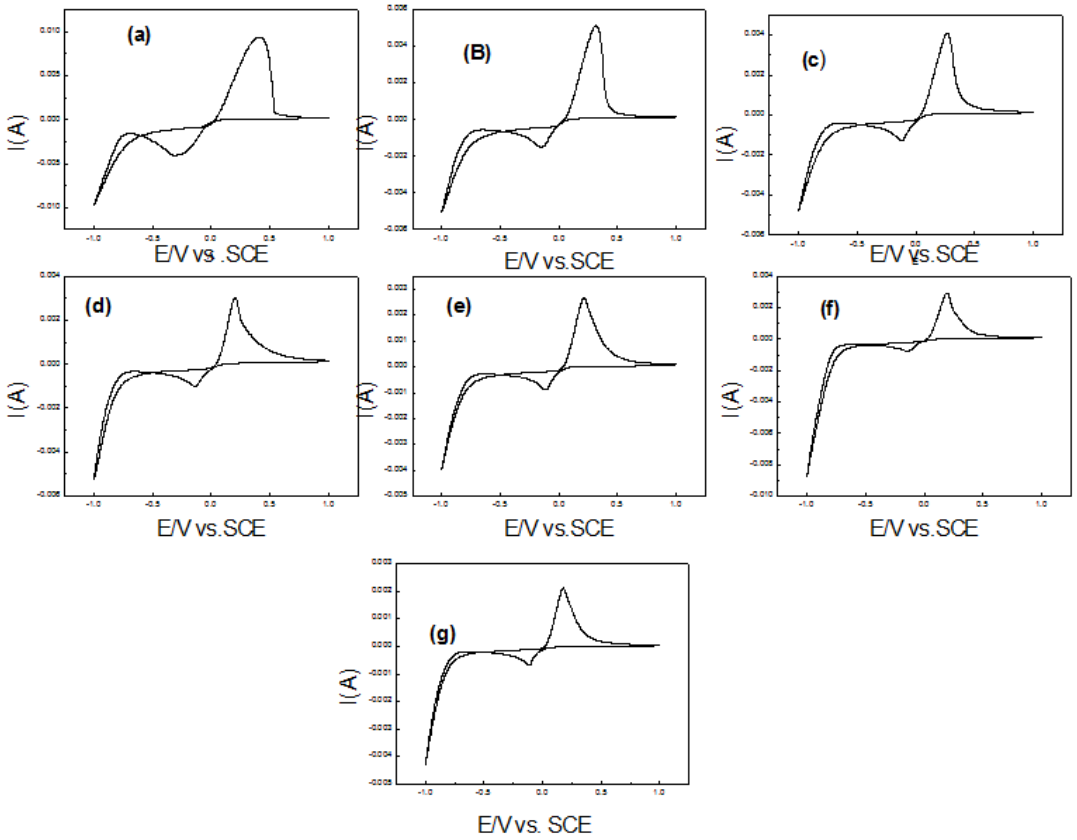

Figure 3. Cyclic voltammetry of Cu-Ni mixed solution after each deposition, from (a) to (g) respectively correspond to samples number used during the deposition process at scan rate 50mv/s

Table 3. V= -0.5 v

Sample number	Volume (mL)	Deposition Time (h)	Quantity of charge (C)	Theoretical quantity of Cu deposited (mol)	Cu concentration ($g \cdot L^{-1}$)		Ni Concentration ($g \cdot L^{-1}$)		Experimental quantity of Cu deposited (mol)	Current efficiency (%)
					Before deposition	After deposition	Before deposition	After Deposition		
0	--	--	--	--	--	--	--	--	--	--
1	150	2	521.1	27.06×10^{-4}	3.6	3.34	1.1	1.08	19.95×10^{-4}	73.72
2	145	2	340.3	17.62×10^{-4}		2.54	1.08	1.08	8.45×10^{-4}	47.95
3	140	2	259.5	13.43×10^{-4}		1.592	1.08	1.10	5.16×10^{-4}	38.42
4	135	2	196.8	10.18×10^{-4}		1.336	1.10	1.11	5.86×10^{-4}	57.56
5	130	2	148.3	7.68×10^{-4}		1.508	1.11	1.12	5.94×10^{-4}	77.34
6	125	2	139.9	7.24×10^{-4}		1.032	1.12	1.11	3.16×10^{-4}	43.64
7	120	2	120.9	6.26×10^{-4}		0.88	1.11	1.12	2.42×10^{-4}	38.65
8	115	2	87.71	4.54×10^{-4}		0.848	1.12	1.10	1.79×10^{-4}	39.42

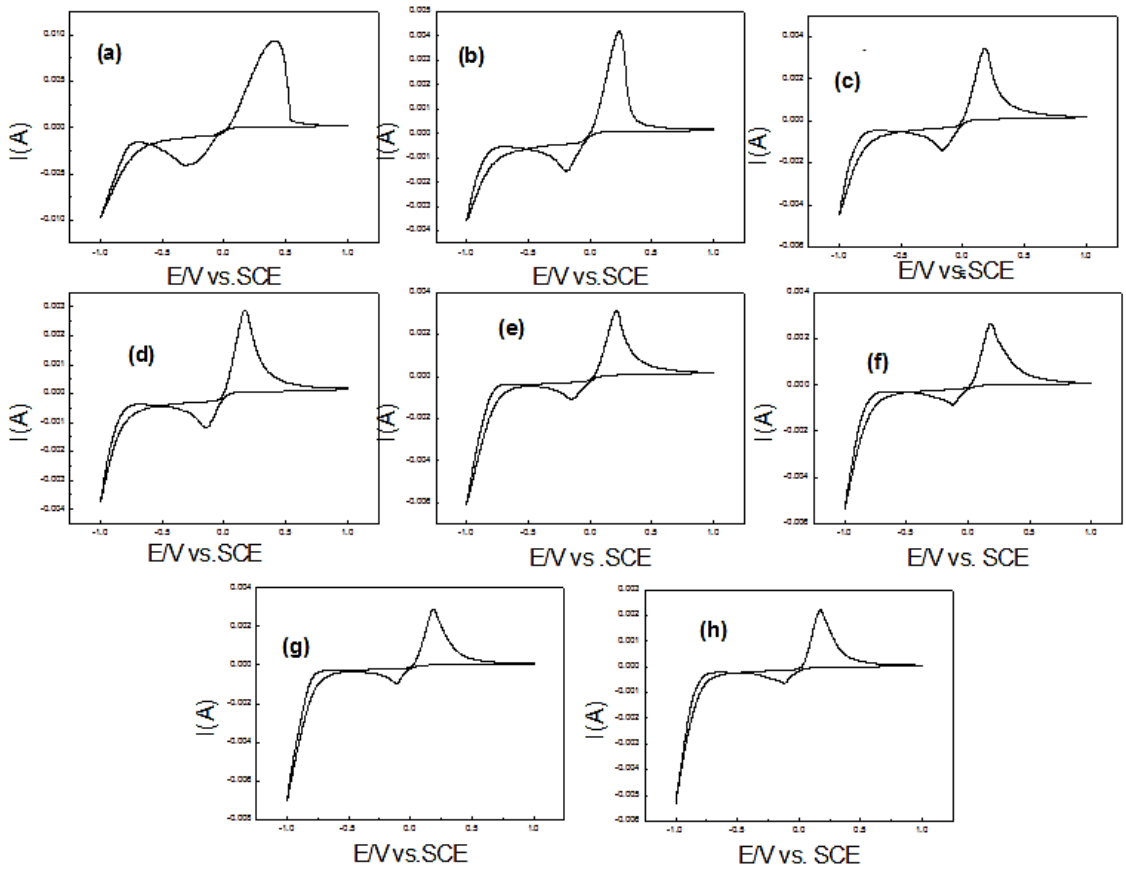

Figure 4. Cyclic voltammetry of Cu-Ni mixed solution after each deposition, from (a) to (h) respectively correspond to samples number used during the deposition process at scan rate 50mv/s